

# CR-SFP: Learning Consistent Representation for Soft Filter Pruning

Jingyang Xiang<sup>1</sup>   Zhuangzhi Chen<sup>2</sup>   Jianbiao Mei<sup>1</sup>   Siqi Li<sup>1</sup>   Jun Chen<sup>1</sup>  
 Yong Liu<sup>1\*</sup>

<sup>1</sup>APRIL Lab, Zhejiang University, Hangzhou, China

<sup>2</sup>IVSN, Zhejiang University of Technology, Hangzhou, China

## Abstract

Soft filter pruning (SFP) has emerged as an effective pruning technique for allowing pruned filters to update and the opportunity for them to regrow to the network. However, this pruning strategy applies training and pruning in an alternative manner, which inevitably causes inconsistent representations between the reconstructed network (R-NN) at the training and the pruned network (P-NN) at the inference, resulting in performance degradation. In this paper, we propose to mitigate this gap by learning consistent representation for soft filter pruning, dubbed as CR-SFP. Specifically, for each training step, CR-SFP optimizes the R-NN and P-NN simultaneously with different distorted versions of the same training data, while forcing them to be consistent by minimizing their posterior distribution via the bidirectional KL-divergence loss. Meanwhile, the R-NN and P-NN share backbone parameters thus only additional classifier parameters are introduced. After training, we can export the P-NN for inference. CR-SFP is a simple yet effective training framework to improve the accuracy of P-NN without introducing any additional inference cost. It can also be combined with a variety of pruning criteria and loss functions. Extensive experiments demonstrate our CR-SFP achieves consistent improvements across various CNN architectures. Notably, on ImageNet, our CR-SFP reduces more than 41.8% FLOPs on ResNet18 with 69.2% top-1 accuracy, improving SFP by 2.1% under the same training settings. The code will be publicly available on GitHub.

## 1. Introduction

In recent years, deep neural networks (DNNs) have achieved remarkable success in a variety of pattern recognition tasks, including image classification [20, 49], object detection [15, 21], semantic segmentation [5, 16] and other fields. However, the great success of DNNs often relies on huge parameters and floating point operations. It

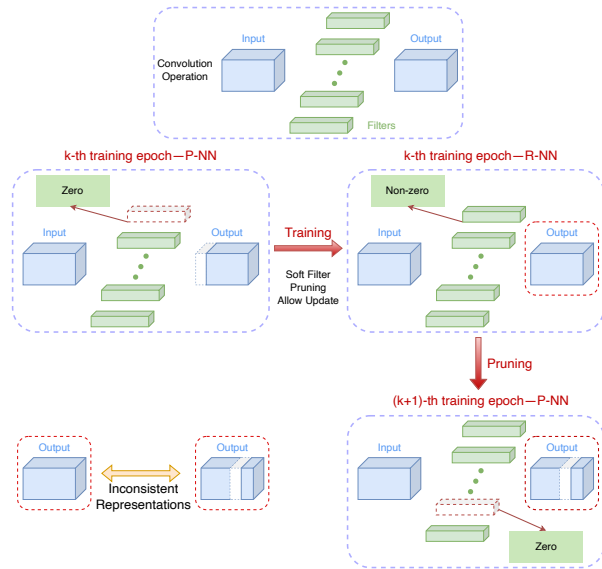


Figure 1. **Inconsistent Representations in the Soft Filter Pruning.** We mark the pruned filters as the red dashed box. SFP allows the pruned filters to be updated during the training process so that the capacity of the model can be recovered. However, SFP trains and prunes network alternately, leading to inconsistent representations in the training and inference stage and hurting the final performance of the model.

hinders them from running in real-time in edge scenarios where computing power and memory are limited, such as smartphones, watches and other wearable devices. In order to balance the trade-off between performance and inference cost, researchers have conducted extensive research on DNNs compression, including low-rank decomposition [6], model pruning [31], model quantization [19], knowledge distillation [24] and efficient architecture design [7, 59].

Among them, model pruning, which reduces memory and computation burden by removing unimportant weights or filters from the model, has received much attention from both industry and academia. In the different prune type, most researchers have paid their attention to filter pruning. Unlike weight pruning, which may still be less efficient in saving inference latency and require dedicated

\*Corresponding author

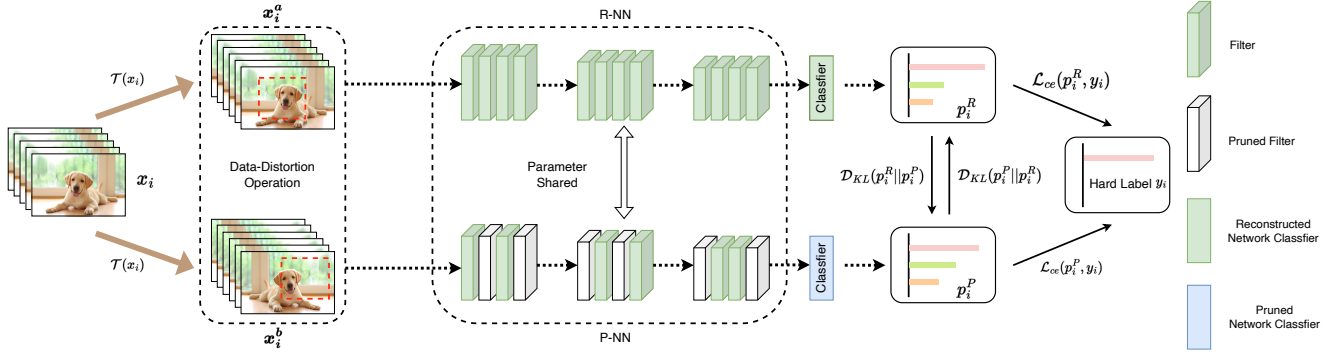


Figure 2. **The overall framework of our proposed CR-SFP.** We take image classification task for illustration. The same input data with different data distortion operations is fed into R-NN and P-NN respectively. R-NN and P-NN share parts of parameters in the backbone and use different classifiers. Both of them are trained with hard label while reducing the representation gap between each other.

software and hardware to achieve actual acceleration, filter pruning removes the entire filter so that it is hardware-friendly and well-compatible with Basic Linear Algebra Subprograms (BLAS) libraries on general-purpose hardware. Therefore, it is easy to achieve realistic acceleration. Filter pruning has been extensively studied, and the current research on filter pruning can mainly be categorized into filter importance measurement [23, 31, 37], pruning process [47], pruning way [22, 26].

In this paper, we focus on the pruning way. According to whether the removed filters can regrow to the network during the training process, the pruning way can be divided into hard filter pruning (HFP) and soft filter pruning (SFP) [22]. For HFP, the pruned filters are permanently removed during the training process. Thus the capacity of the model is reduced, which significantly harms the model’s performance, particularly as the fraction of the network being pruned increases [27]. Most pretrain-prune-finetune (PPF) pipeline for pruning belongs to HFP. HRank [31] is a representative method, which prunes the filter that generates the low rank features and needs hundreds of epochs to finetune. On the contrary, SFP allows the removed filters to be updated with gradients and regrow to the network during the training, preserving the model’s capacity and achieving better performance. Most current SOTA pruning methods are based on the SFP. However, as shown in Fig. 1, the conventional SFP [22] follows the training-pruning pipeline alternately, resulting in inconsistent representations between the reconstructed network (R-NN) during the training and the pruned network (P-NN) during the inference, which hurts final performance of the P-NN.

To address the above-mentioned problem, we propose a novel approach to learn consistent representation for soft filter pruning (CR-SFP). The CR-SFP dynamically prunes the filters in a soft manner while narrowing the gap between P-NN and R-NN to maintain a consistent representation. Particularly, before each training epoch, the filters among

all network layers with minor importance will be selected and set to zero. Then R-NN and P-NN will be trained simultaneously in a parameter-shared manner. This approach avoids introducing a large number of additional training parameters. At the same time, CR-SFP uses bidirectional KL-divergence loss to regularize posterior distribution (class probabilities) in the update. For a mini-batch input, we utilize the same data-distortion operation two times to obtain two-branch distorted samples to train them respectively. It prevents them overfitting the training set and be less effective due to the limitation of valuable information beyond the common hard label [2], while boosting the generalization ability of model [48]. Before the next training epoch, CR-SFP follows the pruning process of the original SFP, where a new set of filters of minor importance is pruned and a part of filters will regrow to network. This pipeline will be alternated during the training process until the network converges. After the last epoch, we export the P-NN and obtain the compact model. The CR-SFP inherits the advantage that SFP can enable the P-NN to have a larger model capacity. Meanwhile, it optimizes R-NN and P-NN simultaneously while achieving consistent representation, thus achieving better performance.

Our main contributions are summarized as follows:

- To address the phenomenon of inconsistent representations of R-NN and P-NN in the SFP during training and inference, we propose to use bidirectional KL-divergence loss to regularize the posterior distribution and achieve consistent representation between them.
- We use different data distortion operations and classifier layers for R-NN and P-NN to enhance the model’s generalization capability and optimize them based on a deep mutual learning pipeline. R-NN and P-NN share a part of the backbone parameters. We only introduce a small number of additional parameters from the classifier layer and keep the training process simple and efficient.
- We have conducted extensive experiments on ImageNet

datasets to validate the effectiveness of our method. For example, our CR-SFP achieves 69.2% top-1 accuracy for ResNet18 with 1.04G FLOPs, suppressing its counterpart SFP by 2.1% under the same training settings.

## 2. Related Work

### 2.1. Network Pruning

Network pruning aims to remove unimportant or redundant parameters in the complex model while preserving the origin performance. In addition to the categorization based on the pruning way described above, the mainstream pruning type can be divided into weight pruning [19], filter pruning [27, 31], weight block pruning [4, 10, 32, 51] and N:M pruning [35, 42] according to their pruning granularity. Filter pruning allows for efficient speedup on general-purpose hardware. The weight pruning is less efficient in memory access and computation, making it difficult to achieve realistic acceleration. Weight block pruning and N:M pruning are semi-structured sparse models proposed in the recent years, both of which can rely on specific hardware or software for efficient acceleration. They are regarded as a promising approach to achieve better trade-offs in inference latency and accuracy compared to weight pruning or filter pruning. On the other hand, identifying important weights/filters/blocks is also an important aspect. Although most of the work uses filter norm, absolute magnitude of weight, or scaling factors in batch normalization as pruning criteria, there are also some studies on importance measurement. For example, FPGM [23] proposes to use the geometric median of filters to estimate the importance of filters. The first-order Taylor expansion [37, 38], second-order derivatives [8, 41, 62] have also been proposed to approximate the loss change after pruning. In order to obtain pruned networks more efficiently, researchers also investigate progressive pruning [26], pruning at initialized [25] to replace the complicate pretrain-pruning-finetune [31] pruning pipeline and these methods also obtain good results.

### 2.2. Consistent Training

Our work aims to learn consistent representation between R-NN and P-NN, which also relates to a few works of consistent training. From a structure perspective, the most representative methods are ELD [33], FD [63] and R-Drop [55]. Specifically, the purpose of ELD is to reduce the gap between the dropout-enabled sub-model during training and the full model without dropout during inference, while FD works to enhance the representation consistency between the two sub-models. Both ELD and FD adopt the  $\ell_2$ -norm to align the hidden space. Different from them, R-Drop utilizes bidirectional KL-divergence loss to regularize the posterior distribution between the two sub-models, which improves the consistency of representation more ef-

fectively, and it also proves this constraint can improve the representation consistency of the model during the training and inference. From a data perspective, DNNs with good generalization ability should exhibit similar posterior distributions for different data distortion operations of the same input data [48]. DDGSD [56] excavates the potential capacity of a single network by learning consistent global feature distributions and posterior distributions across these distorted versions of data. Cutoff [46] discards part of the information within an input sentence to yield its restricted views and use them to enhance the consistency training. To learn more consistent representation from data, researchers also have designed some new loss terms to enforce the features toward intra-class compactness and inter-class separability, such as contrastive loss [18], triplet loss [45] and center loss [54].

### 2.3. Knowledge Distillation

Minimizing the KL-divergence between the posterior distributions of teacher and student models is closely associated with knowledge distillation [1, 12, 24]. Knowledge distillation improves the final performance of the student network by pre-training the teacher and then guiding the student or co-training the teacher and student. In our setting, the teacher and student are the R-NN and P-NN, respectively. R-NN and P-NN share a part of backbone weights in the network and use different classifier layers for themselves. Thus it resembles both self-knowledge distillation [36, 56] and online knowledge distillation [60] scenario. However, different from previous work, which aimed at improving the performance of the dense network by exploring dark knowledge from itself or distilling knowledge between layers [17, 58], our work focuses on obtaining better P-NN from R-NN by learning consistent representation between them. Moreover, unlike most previous methods, which introduce auxiliary networks and increase the complexity of the training process in need of large memory and time cost, our method only requires a single network via a parameter-shared approach, which is simple and efficient.

## 3. Methodology

In this section, we will firstly introduce the symbol and annotations to define a convolutional neural network (CNN) and training procedure to SFP. Then we will describe consistent learning process to our CR-SFP. Finally, we will show how to obtain compact model.

### 3.1. Preliminaries

Without loss of generality, we consider a DNN with  $L$  CNN layers. We parameterize the weights in the CNN as  $\mathbf{W} = \{\mathbf{W}^1, \dots, \mathbf{W}^L\}$ , where  $\mathbf{W}^l \in \mathbb{R}^{C_{out}^l \times C_{in}^l \times K_h^l \times K_w^l}$  is the weight for  $l$ -th layer of the network.  $C_{out}^l$ ,  $C_{in}^l$ ,  $K_h^l$  and  $K_w^l$

denote the output channel, input channel, kernel height and kernel width of the  $l$ -th layer respectively. The shapes of input tensor  $\mathbf{X}^l$  and output tensor  $\mathbf{X}^{l+1}$  are  $C_{in}^l \times H_l \times W_l$  and  $C_{out}^l \times H_{l+1} \times W_{l+1}$ . The convolutional operation of the  $j$ -th filter in the  $l$ -th layer can be written as:

$$\mathbf{X}_j^{l+1} = \mathbf{W}_j^l * \mathbf{X}^l \quad (1)$$

where  $\mathbf{W}_j^l \in \mathbb{R}^{C_{in}^l \times K_h^l \times K_w^l}$  represents the  $j$ -th filter of  $l$ -th CNN layer. and  $\mathbf{W}^l$  consists of  $\{\mathbf{W}_1^l, \dots, \mathbf{W}_{C_{out}^l}^l\}$ . The  $\mathbf{X}_j^{l+1}$  represents the  $j$ -th output feature map of the  $l$ -th layer. For simplify, we omit the normalization and activation layers of the network. In the Sec. 3.3, we will describe how to deal with them to obtain compact model.

In order to obtain P-NN during the training, we introduce an output filter mask  $\mathbf{m}^l \in \{0, 1\}^{C_{out}^l}$  which is updated according to the pruning action for layer  $l$ . Using these masks, we define the forward propagation of P-NN as:

$$\mathbf{X}_j^{l+1} = (\mathbf{W}_j^l \odot \mathbf{m}_j^l) * \mathbf{X}^l = \hat{\mathbf{W}}_j^l * \mathbf{X} \quad (2)$$

where  $\mathbf{m}_j^l$  denotes whether the  $j$ -th filter is pruned.  $\mathbf{m}_j^l$  will be broadcasted to match the shape of  $\mathbf{W}_j^l$ .

SFP divides the pruning pipeline into three steps: filter selection, pruning and reconstruction. Specifically, during the filter selection stage, SFP evaluates the importance of each filter based on specific criteria. Assume that the pruning rate of the  $l$ -th layer is  $P^l$ . In the filter pruning stage, we select the lowest important  $C_{out}^l P^l$  filters by  $\mathcal{I}(\mathbf{W}^l)$  and set them to zero to temporarily eliminate their contribution to the network output. Unlike HFP, which permanently removes the pruned filters, SFP allows the pruned filters to be reconstructed (e.g. updated from zero) by the forward-backward process and regrow to the network. The SFP repeats these steps alternately during the whole training process, dynamically removes the filters and finally exports a compact and efficient model.

In this paper we use the  $\ell_2$ -norm to measure the importance of each filter:

$$\mathcal{I}(\mathbf{W}_j^l) = \sqrt{\sum_{n=1}^{C_{in}^l} \sum_{k_1=1}^{K_h^l} \sum_{k_2=1}^{K_w^l} |\mathbf{W}_j^l(n, k_1, k_2)|^2} \quad (3)$$

Meanwhile, we use the same pruning rate  $P^l = P$  for each layer to reduce hyper-parameters. It's worth noting that our approach applies equally to other criteria or cases where different layers have different pruning rates.

### 3.2. Consistent Representation

We define the training set  $\mathcal{S} = \{(x_1, y_1), \dots, (x_N, y_N)\}$  as a labeled source dataset, where  $N$  is the total number of training samples and  $y_i$  is the corresponding hard label. Then

the optimization objection for P-NN  $\phi(x_i; \mathbf{W}, \mathbf{m})$  can be formulated as:

$$\operatorname{argmin}_{\mathbf{W}, \mathbf{m}} \frac{1}{N} \sum_{i=1}^N \mathcal{L}_{ce}(\phi(x_i; \mathbf{W}, \mathbf{m}), y_i) \quad (4)$$

where  $\mathcal{L}_{ce}$  is the cross-entropy loss.

Conventional SFP [22] optimizes Eq. (4) via minimizing the loss for R-NN  $\phi(x_i; \mathbf{W}, \mathbf{1})$  via:

$$\operatorname{argmin}_{\mathbf{W}, \mathbf{m}} \frac{1}{N} \sum_{i=1}^N \mathcal{L}_{ce}(\phi(x_i; \mathbf{W}, \mathbf{1}), y_i) \quad (5)$$

which neglects the representation gap between P-NN and R-NN and inevitably hurts the performance to P-NN.

To address the above-mentioned problem, we propose CR-SFP in this paper, a simple but effective framework to learning consistent representation for P-NN and R-NN. The overall framework of our method is shown in Fig. 2. Specifically, for the one training step, we sample a mini-batch input  $B = \{(x_1, y_1), \dots, (x_n, y_n)\}$  from training set  $\mathcal{S}$  and apply the same data-distortion operation  $\mathcal{T}(B)$  two twice to obtain two-branch distorted samples  $B^a = \{(x_1^a, y_1), \dots, (x_n^a, y_n)\}$  and  $B^b = \{(x_1^b, y_1), \dots, (x_n^b, y_n)\}$ , where the hard labels  $\{y_1, \dots, y_n\}$  are shared for them. Then,  $B^a$  and  $B^b$  are fed into R-NN and P-NN to get corresponding outputs and their cross entropy loss:

$$\begin{cases} p_i^R = \operatorname{softmax}(\phi(x_i^a; \mathbf{W}, \mathbf{m})), i = 1, \dots, n \\ p_i^P = \operatorname{softmax}(\phi(x_i^b; \mathbf{W}, \mathbf{1})), i = 1, \dots, n \\ \mathcal{L}_{ce} = \frac{1}{n} \sum_{i=1}^n \mathcal{L}_{ce}(p_i^R, y_i) + \mathcal{L}_{ce}(p_i^P, y_i) \end{cases} \quad (6)$$

To reach the consistent posterior representation between the two-branch distorted versions, following the previous works [55, 60], CR-SFP adopts the bi-directional KL divergence to measure the match as follows:

$$\mathcal{L}_{KL} = \frac{1}{2n} \sum_{i=1}^n \mathcal{D}_{KL}(p_i^R || p_i^P) + \mathcal{D}_{KL}(p_i^P || p_i^R) \quad (7)$$

where

$$\mathcal{D}_{KL}(p_1 || p_2) = - \sum p_1 \log p_2 + \sum p_1 \log p_1 \quad (8)$$

Similar to [3, 60], we implement stopgrad operation by modifying Eq. (8) as:

$$\mathcal{D}_{KL}(\operatorname{stopgrad}(p_1) || p_2) \quad (9)$$

This means that  $p_1$  is treated as a constant in this term and the gradient to  $\partial \mathcal{D}_{KL}(p_1 || p_2) / \partial p_1$  is zero.

Our CR-SFP mainly consists of two types of loss terms to update parameters of single network:

$$\mathcal{L}_{net} = \mathcal{L}_{ce} + \lambda \mathcal{L}_{KL} \quad (10)$$

where  $\lambda$  is bi-directional KL-divergence loss weight for posterior distribution regularization. The first term of Eq. (10) are the supervised losses of R-NN and P-NN. We improve their performance by simultaneously optimizing the corresponding parameters of both networks in a parameter-shared manner. The last term aims to improve the consistency of the R-NN and P-NN representation and further enhance the performance to P-NN.

### 3.3. Obtaining Compact Model

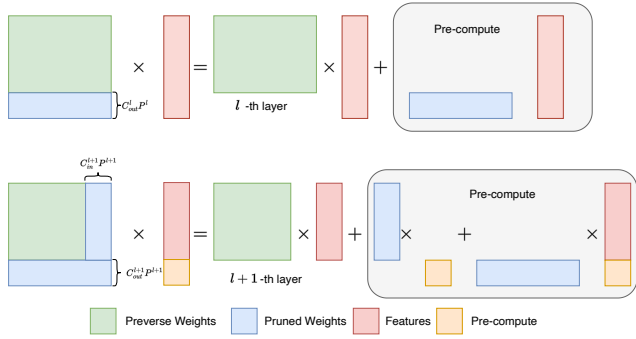


Figure 3. **Pipeline for obtaining compact model.** We omit the BN and act layer for simplify.

Pruning filters is equivalent to removing corresponding the output feature maps in the  $l$ -th layer. Although the presence of the normalization and activation layer between the  $l$ -th and the  $l + 1$ -th convolutional layer may result in a non-zero feature map, these values can be pre-computed and merged into the  $l + 1$ -th normalization layer during the inference process without introducing additional overhead. Thus, as the output channel of the  $l$ -th convolutional layer is reduced from  $C_{out}^l$  to  $C_{out}^l(1 - P^l)$ , the input channel of the  $l + 1$ -th convolutional layer will also be reduced from  $C_{in}^{l+1}$  to  $C_{in}^{l+1}(1 - P^l)$ . In this case, the computational cost of the model will be significantly reduced and we can achieve an efficient acceleration ratio.

Here we give specific steps for obtaining compact model as shown in Fig. 3. Assuming that we complete the pruning of  $l$ -th convolutional layer, we can split its weights  $\mathbf{W}^l$  into the pruned weights  $\mathbf{W}_p^l$  and the retained weights  $\mathbf{W}_r^l$ , where  $\mathbf{W}^l = [\mathbf{W}_p^l; \mathbf{W}_r^l]$ . Based on [42], we can know our description is not out of generality. The forward propagation of the  $l$ -th layer can be written as:

$$\mathbf{X}^{l+1} = [\mathbf{X}_p^{l+1}; \mathbf{X}_r^{l+1}] = [\mathbf{W}_p^l * \hat{\mathbf{X}}^l; \mathbf{W}_r^l * \hat{\mathbf{X}}^l] \quad (11)$$

where  $\mathbf{X}_p^{l+1}$  and  $\mathbf{X}_r^{l+1}$  are the corresponding features for  $\mathbf{W}_p^l$  and  $\mathbf{W}_r^l$  respectively.

### Algorithm 1: Algorithm Description of CR-SFP

- 1 **Input:** training data:  $\mathcal{S}$ , pruning rate:  $P$ , total training epochs  $epoch_{max}$  ;
- 2 **Parameter:** model parameters  $\mathbf{W} = \{\mathbf{W}^1, \dots, \mathbf{W}^L\}$ , filter masks  $\mathbf{m} = \{\mathbf{m}^1, \dots, \mathbf{m}^L\}$  ;
- 3 **Output:** the pruned model and its parameters  $\mathbf{W}^*$
- 4 **for**  $epoch = 1; epoch \leq epoch_{max}; epoch ++$  **do**
- 5     Update the model parameter  $\mathbf{W}$  based on Eq. (10) ;
- 6     **for**  $l = 1; l \leq L; l ++$  **do**
- 7         Get the  $\mathcal{I}(\mathbf{W}_j^l)$  for each filter,  $1 \leq j \leq C_{out}^l$  ;
- 8         Zeroize  $C_{out}^l P$  filters by  $\mathcal{I}(\mathbf{W}_j^l)$  filter selection ;
- 9         Update  $\mathbf{m}^l$  based by  $\mathcal{I}(\mathbf{W}_j^l)$  filter selection ;
- 10    Reformat  $\mathbf{W}$  to  $\mathbf{W}^*$  based on Eq. (11) to Eq. (14) ;
- 11 **return** the pruned model and its parameters  $\mathbf{W}^*$  ;

We assume that the convolutional layer is followed by the batch normalization (BN) and activation (act) layer, then  $\hat{\mathbf{X}}^k = \text{act}(\text{BN}(\mathbf{X}^k))$ . The forward propagation of the  $l$ -th layer can be written as:

$$\begin{aligned} \hat{\mathbf{X}}^{l+1} &= \text{act}(\text{BN}(\mathbf{X}^{l+1})) \\ &= [\text{act}(\text{BN}(\mathbf{X}_p^{l+1})) ; \text{act}(\text{BN}(\mathbf{X}_r^{l+1}))] \quad (12) \\ &= [\hat{\mathbf{X}}_p^{l+1}; \hat{\mathbf{X}}_r^{l+1}] \end{aligned}$$

Since we prune the weights  $\mathbf{W}_p^l$ ,  $\mathbf{X}_p^{l+1}$  is equal to zero and the parameters in BN and act are known ahead of time, we can pre-compute  $\hat{\mathbf{X}}_p^{l+1}$  in the process of inference.

For the forward propagation in the  $l + 1$ -th layer:

$$\begin{aligned} \mathbf{X}^{l+2} &= [\mathbf{X}_p^{l+2}; \mathbf{X}_r^{l+2}] = [\mathbf{W}_p^{l+1} * \hat{\mathbf{X}}^{l+1}; \mathbf{W}_r^{l+1} * \hat{\mathbf{X}}^{l+1}] \\ &= [\mathbf{W}_p^{l+1} * \hat{\mathbf{X}}^{l+1}; \mathbf{W}_r^{l+1} * [\hat{\mathbf{X}}_p^{l+1}; \hat{\mathbf{X}}_r^{l+1}]] \quad (13) \end{aligned}$$

Based on the additivity of the convolution, we can get:

$$\begin{aligned} &\mathbf{W}_r^{l+1} * [\hat{\mathbf{X}}_p^{l+1}; \hat{\mathbf{X}}_r^{l+1}] \\ &= [\mathbf{W}_{r_1}^{l+1}; \mathbf{W}_{r_2}^{l+1}] * [\hat{\mathbf{X}}_p^{l+1}; \hat{\mathbf{X}}_r^{l+1}] \quad (14) \\ &= \mathbf{W}_{r_1}^{l+1} * \hat{\mathbf{X}}_p^{l+1} + \mathbf{W}_{r_2}^{l+1} * \hat{\mathbf{X}}_r^{l+1} \end{aligned}$$

where  $\mathbf{W}_{r_1}^{l+1}$  and  $\mathbf{W}_{r_2}^{l+1}$  represent the corresponding indices of the  $l + 1$ -th layer weight along the input channel based on the pruning results of the  $l$ -th layer. Since  $\mathbf{W}_{r_1}^{l+1} * \hat{\mathbf{X}}_p^{l+1}$  in the Eq. (14) can also be pre-computed and integrated into BN layer after the  $l + 1$ -layer, we can also remove the corresponding input channels and repeat this process to obtain a compact model.

The details of CR-SFP are explained in Algorithm 1.

Model	Method	PT	FLOPs	Parameters	Top-1	Top-5	Epochs
ResNet18	MIL [9]	N	1.17G	N/A	66.3%	86.9%	200
	SFP [22]	N	1.04G	6.53M	67.1%	87.8%	100
	FPGM [23]	N	1.04G	6.53M	67.8%	88.1%	100
	PFP [30]	Y	1.27G	6.57M	67.4%	87.9%	270
	<b>CR-SFP (Ours)</b>	<b>N</b>	<b>1.04G</b>	<b>6.53M</b>	<b>69.2%</b>	<b>88.9%</b>	<b>100</b>
ResNet34	SFP [22]	N	2.2G	11.10M	71.8%	90.3%	100
	FPGM [23]	Y	2.2G	11.10M	72.6%	91.1%	200
	DMC [13]	Y	2.1G	N/A	72.6%	91.1%	490
	SCOP [52]	Y	2.0G	11.86M	72.6%	91.0%	230
	CHEX [26]	N	2.0G	15.43M	73.5%	N/A	250
	NPPM [14]	Y	2.1G	N/A	73.0%	N/A	390
	W-Gates [29]	Y	2.1G	N/A	72.7%	N/A	210
	HTP-URC [43]	Y	2.1G	12.00M	73.0%	N/A	200
	<b>CR-SFP (Ours)</b>	<b>N</b>	<b>2.2G</b>	<b>11.10M</b>	<b>73.0%</b>	<b>91.1%</b>	<b>100</b>
ResNet50	SFP [22]	N	2.3G	15.93M	74.6%	92.9%	100
	FPGM [23]	Y	2.3G	15.93M	75.6%	92.9%	200
	SCOP [52]	Y	2.2G	14.62M	76.0%	92.8%	230
	EagleEye [28]	Y	2.0G	N/A	76.4%	92.9%	240
	Taylor [38]	Y	2.3G	14.20M	74.5%	N/A	125
	DSA [39]	N	2.0G	N/A	74.7%	92.1%	120
	While-Box [61]	N	2.2G	N/A	75.3%	92.4%	190
	W-Gates [29]	Y	2.3G	N/A	75.7%	92.6%	210
	TPP [53]	Y	2.5G	N/A	76.4%	N/A	190
	DepGraph [11]	Y	2.0G	12.46M	75.8%	N/A	190
<b>CR-SFP (Ours)</b>	<b>N</b>	<b>2.3G</b>	<b>15.93M</b>	<b>76.6%</b>	<b>93.1%</b>	<b>100</b>	

Table 1. **Comparison of pruning ResNet on ImageNet.** In “FT” column, “Y” and “N” indicate whether requiring the pre-trained model as initialization or not. We report FLOPs, Parameters, top-1 and top-5 accuracy of pruned model. “Epoch” are reported as: pretraining epochs (if needed) plus all subsequent training epochs to obtain the final pruned model.

## 4. Experiments

### 4.1. Benchmark Datasets and Network Structure

In order to investigate the effectiveness of our CR-SFP, we adopt ImageNet [44] as a benchmark dataset. ImageNet is a large-scale dataset for image classification tasks, containing 1.28 million training images and 50,000 validation images with 1000 classes. Following previous works, we focus on pruning the challenging ResNet models with different depths in this paper, including ResNet18, ResNet34, and ResNet50. The baseline ResNet-18/34/50 models have 1.8/3.7/4.1 GFLOPs.

**Experimental Settings.** Following the previous work SFP [22] and FPGM [23], our network is trained from scratch rather than initialized on a pre-trained model. We use stochastic gradient descent (SGD) for all experiments with momentum of 0.9 and weight decay  $1e-4$  to optimize the training objective. The initial learning rate is set to 0.1 for the total batch size of 256. All networks are trained for 100 epochs and the learning rate is reduced by a multiple of 0.1 at 30,60 and 90 epochs respectively. For data aug-

mentation, we only apply random crops, horizontal flip, and normalization. All experiments run on PyTorch [40] framework with NVIDIA RTX3090 GPUs using AMP (automatic mixed precision). We calculate FLOPs by counting multiplication and addition as one operation following He [20].

To keep our method simple and generic, we set  $\lambda = 0.2$  to the bidirectional KL-divergence loss in Eq. (10) to all experiments unless otherwise stated. At the same time, we did not try to adjust potential strategies such as the criterion of filter importance and the pruning interval epoch. For different networks and datasets, their optimal values can be obtained using grid search with others fixed. In this paper, though they are not optimal, we still achieved competitive results with current state-of-the-art methods.

### 4.2. ResNet on ImageNet

Same with SFP [22], we prune ResNet models with the same pruning rate across layers and do not prune the shortcut branch for simplification.

Tab. 1 shows the experiment results for the ImageNet dataset. CR-SFP shows excellent performance with ResNet

Method	Top-1	Top-5
$\mathcal{L}_{ce}(y_i, \hat{p}_i^R)$ (SFP Baseline)	67.1%	87.8%
+ $\mathcal{L}_{ce}(y_i, \hat{p}_i^P) + 0.2\mathcal{D}(\hat{p}_i^R, \hat{p}_i^P)$	68.6%	88.3%
+ Data Distortion ( <b>default</b> )	69.2%	88.9%
+ Advanced Training Recipe	69.5%	89.1%

Table 2. Ablation study of different components in CR-SFP. Advanced training recipe means cosine LR schedule and longer training epochs (200 epochs).

Method	Baseline		Pruned	
	Top-1	Top-5	Top-1	Top-5
SFP (Baseline)	69.8%	89.1%	68.0%	88.1%
<b>CR-SFP (Ours)</b>	69.8%	89.1%	69.3%	88.8%

Table 3. Results starting from the pretrained models.

models of different depths. For ResNet18, CR-SFP can achieve 69.2% top-1 accuracy with only 100 training epochs, exceeding SFP 2.1%. Moreover, it exceeds PFP by 1.8% top-1 accuracy, despite PFP having 1.27G FLOPs and a total of 270 training epochs. The results show that CR-SFP not only inherits the advantage that SFP can maintain the model’s capacity but also improves the convergence speed by learning consistent representation of R-NN and P-NN, thus achieving better results with the same training epoch. For ResNet34 and ResNet50, CR-SFP achieves competitive results with fewer epochs than the previous state-of-the-art methods. Moreover, our method only needs to be trained from scratch, avoiding the complex process of training, pruning, and fine-tuning pipeline required by pre-training-based methods like [28, 29, 43, 61].

We do not adopt advanced training recipes on CR-SFP, such as cosine LR schedule, more extensive epochs or data augmentation such as mixup [57] in Tab. 1. From Sec. 4.3, we can see by applying these training recipes, our approach achieves better results.

### 4.3. Ablation Analysis

We use ablation analysis to investigate the effectiveness of different components in the CR-SFP. All the following results are based on pruning the ResNet18 model to 1.04G FLOPs on the ImageNet.

**Component Study.** In Tab. 2, we study the effectiveness of different components in CR-SFP. The baseline is SFP [22], where the model is pruned by minimize Eq. (5).

Firstly, we apply the same data distortion operation for the input data with Eq. (10), i.e.,  $x_i^a = x_i^b$ . This mutual learning process brings in 0.6% top-1 accuracy for improvement. When the different data distortion operations are applied, instead of sticking to the fixed input distributions during the whole training, we can obtain a P-NN with a

Prune Criterion	SFP (Baseline)		CR-SFP (Ours)	
	Top-1	Top-5	Top-1	Top-5
$\ell_2$ -norm	67.1%	87.8%	69.2%	88.9%
Geometric Median	67.8%	88.1%	69.3%	88.9%
Taylor FO	67.5%	88.0%	69.0%	88.8%

Table 4. Comparison with different pruning criterion.

Distance Function	Top-1	Top-5
KL-Divergence	69.2%	88.9%
Cosine-Similarity	68.9%	88.4%
Binary-Crossentropy	68.7%	88.5%

Table 5. Comparison with different distance function.

stronger consistent representation with the R-NN. It further improves the top-1 and top-5 accuracy by 0.3% and 0.2% respectively. Following previous methods [26, 50] which applied more advanced training recipes for the pruning, we use a cosine LR schedule and longer training epochs (200 epochs), prompting better model convergence. Benefiting from the advanced training recipes, we achieve 69.5% top-1 accuracy, further outperforming existing methods.

**CR-SFP from Pretrained Models.** To further demonstrate the generality of our CR-SFP, we use the pre-trained ResNet18 weight to initialize the model. We adopt the ResNet18 weights from torchvision [34] model zoo for a fair comparison. We perform 100 epochs of pruning on both SFP and CR-SFP. As shown in Tab. 3, our method achieves 1.3% top-1 accuracy improvement than the original SFP when under the same training settings and reducing the same amount of FLOPs. What is more, comparing Tab. 2 and Tab. 3, we find that with the same training epoch (200 versus 100+100), our method can obtain better results (69.5% versus 69.3%) when trained from scratch than pretrain, prune and finetune pipeline.

**Pruning Criterion.** To validate the effectiveness of CR-SFP, we apply this training framework to the different pruning criteria, including  $\ell_2$ -norm, Geometric Median [23], Taylor FO [38] and compare their final accuracy in Tab. 4. We observe that CR-SFP is robust to the pruning criterion, as it improves the accuracy for all three criteria. For example, with only 100 training epochs, CR-SFP with Geometric Median achieves 69.3% top-1 accuracy, which further suppresses the results in Tab. 1. This suggests the learning of consistent representation and the study of prune criterion are vertical, and the two can be mutually enhanced to achieve better results.

**Distance Function.** We study the influence of distance function  $\mathcal{D}$  to our CR-SFP, including bidirectional KL-divergence, negative cosine similarity and binary cross-

$\lambda$	Top-1	Top-5	$\lambda$	Top-1	Top-5
-0.5	65.5%	86.4%	0.2	<b>69.2%</b>	<b>88.9%</b>
-0.2	68.3%	88.1%	0.5	68.9%	88.6%
-0.1	68.5%	88.2%	1	68.9%	88.4%
0	68.6%	88.3%	2	68.4%	88.2%
0.1	68.8%	88.6%	5	66.6%	87.1%

Table 6. Comparison with different weight  $\lambda$ .

entropy. All hyper-parameters and architectures are unchanged and the operation of stopgrad is also applied as mentioned above, though they may be sub-optimal for this.

As can be seen in Tab. 5, our method works even better with KL-divergence, which bring 0.3% and 0.5% top-1 accuracy improvement respectively compared to negative cosine similarity and binary cross-entropy. Since different distance functions should correspond using different hyper-parameters, we consider it is normal for cosine similarity and binary cross-entropy to outperform KL-divergence with default settings. As previous distillation methods have often used KL-divergence as a loss function to regularize the posterior probability distribution, we adopt it as default in this paper. We believe that better results can be achieved by choosing appropriate hyper-parameters based on specific distance functions.

**Effect of Weight  $\lambda$ .** Further, we investigate the impact of the bidirectional KL-divergence loss weight  $\lambda$ . Here, we conduct experiments by varying the  $\lambda$  in Tab. 6. For ResNet18, small  $\lambda$  often brings better results and  $\lambda = 0.2$  is the best which achieves 69.2% top-1 accuracy. Too much regularization is not good because it will make network ignore information from labels and top-1 accuracy drops to 66.6% when  $\lambda$  is set to 5. We also set  $\lambda = -0.1, -0.2, -0.5$  respectively to enhance the inconsistency of R-NN and P-NN. It only gets 65.5% top-1 accuracy with  $\alpha = -0.5$ , which indicates the importance of consistent representation. Although  $\lambda = -0.1$  and  $\lambda = -0.2$  also achieve good results, they are still down compared to  $\lambda = 0$ . We believe this is due to the fact that although these settings enhance inconsistency leading to performance degradation, they still achieve reasonable results due to strong monitoring of supervised losses  $\mathcal{L}_{ce}$ . Note the choice of  $\lambda$  should be related to the degree of model inconsistency and the model’s ability to fit the data. Therefore, adopting a more appropriate  $\lambda$  for different models and datasets should yield better results.

## 5. Cost Analysis

Compared to the conventional SFP procedure, our implementation needs to forward batch data twice at each training step. One potential limitation is that the computational increases at each step. Hence, we plot the imagenet validation accuracy curves along the training epoch of SFP, SFP with a doubled batch size and CR-SFP. We implement dou-

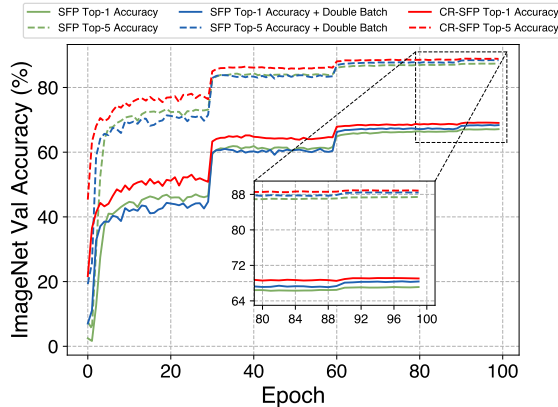


Figure 4. ImageNet val accuracy of SFP, SFP with a doubled batch size and CR-SFP. Top-1 and Top-5 accuracy are reported.

ble batch size by applying input data  $B$  with two twice data distortion operations and concatenating them to  $[B^a; B^b]$  in the same mini-batch to forward once. This is similar to enlarging the epochs to be double at training stage. The difference is that half of the data in doubled batch size are the same as the other half, while directly doubling the training epoch, the data in the same mini-batch are all different. The curves are shown in Fig. 4. We can see that double batch size can also achieve improvement to SFP (68.4% top-1 accuracy) while it still falls behind our CR-SFP (69.2% top-1 accuracy). Meanwhile, we also test the training speed. For the detailed training speed for each step, we present the number here: SFP + Double Batch costs near 214ms per step, CR-SFP costs about 218ms per step. The additional time cost comes from the KL-divergence loss backward computation, which is only 4ms and almost negligible. From the above analysis, we can know CR-SFP is an efficient framework and improves the performance to a stronger one with similar training costs.

## 6. Conclusions

SFP is an effective way to enhance the performance of pruning networks. This paper focuses on solving the inconsistent representation problem of R-NN and P-NN during the training process. Specifically, we propose learning consistent representation for soft filter pruning (CR-SFP). During the training procedure, CR-SFP optimizes R-NN and P-NN simultaneously in a parameter-shared manner. Meanwhile, it improves their consistency by minimizing the posterior probability distribution from different data-distorted versions with bidirectional KL-divergence loss. During the inference, we can export P-NN without introducing any additional computational costs. CR-SFP is an effective and efficient method which not only inherits the advantage of SFP that can preserve model capacity but also improves the performance of P-NN. In the case of limited training epochs, extensive experiments have demonstrated that CR-SFP can



achieve competitive or superior results compared to state-of-the-art methods. Furthermore, transferring the consistent representation learning to other scenarios, such as binary neural networks (binary weights versus full precision weights), will be further studied in our future work.

## References

- [1] Zeyuan Allen-Zhu and Yuanzhi Li. Towards understanding ensemble, knowledge distillation and self-distillation in deep learning. In *The Eleventh International Conference on Learning Representations*, 2023. 3
- [2] Rohan Anil, Gabriel Pereyra, Alexandre Passos, Robert Ormandi, George E Dahl, and Geoffrey E Hinton. Large scale distributed neural network training through online distillation. *arXiv preprint arXiv:1804.03235*, 2018. 2
- [3] Xinlei Chen and Kaiming He. Exploring simple siamese representation learning. In *Proceedings of the IEEE/CVF conference on computer vision and pattern recognition*, pages 15750–15758, 2021. 4
- [4] Zhuangzhi Chen, Jingyang Xiang, Yao Lu, Qi Xuan, Zhen Wang, Guanrong Chen, and Xiaoniu Yang. Rgp: Neural network pruning through regular graph with edges swapping. *IEEE Transactions on Neural Networks and Learning Systems*, pages 1–13, 2023. 3
- [5] Ioana Croitoru, Simion-Vlad Bogolin, and Marius Leordeanu. Unsupervised learning of foreground object segmentation. *International Journal of Computer Vision (IJCV)*, 127(9):1279–1302, 2019. 1
- [6] Emily L Denton, Wojciech Zaremba, Joan Bruna, Yann LeCun, and Rob Fergus. Exploiting linear structure within convolutional networks for efficient evaluation. *Advances in neural information processing systems*, 27, 2014. 1
- [7] Xiaohan Ding, Xiangyu Zhang, Ningning Ma, Jungong Han, Guiguang Ding, and Jian Sun. Repvgg: Making vgg-style convnets great again. In *Proceedings of the IEEE/CVF conference on computer vision and pattern recognition*, pages 13733–13742, 2021. 1
- [8] Xin Dong, Shangyu Chen, and Sinno Pan. Learning to prune deep neural networks via layer-wise optimal brain surgeon. *Advances in neural information processing systems*, 30, 2017. 3
- [9] Xuanyi Dong, Junshi Huang, Yi Yang, and Shuicheng Yan. More is less: A more complicated network with less inference complexity. In *Proceedings of the IEEE conference on computer vision and pattern recognition*, pages 5840–5848, 2017. 6
- [10] Erich Elsen, Marat Dukhan, Trevor Gale, and Karen Simonyan. Fast sparse convnets. In *Proceedings of the IEEE/CVF conference on computer vision and pattern recognition*, pages 14629–14638, 2020. 3
- [11] Gongfan Fang, Xinyin Ma, Mingli Song, Michael Bi Mi, and Xinchao Wang. Depgraph: Towards any structural pruning. In *Proceedings of the IEEE/CVF Conference on Computer Vision and Pattern Recognition*, pages 16091–16101, 2023. 6
- [12] Tommaso Furlanello, Zachary Lipton, Michael Tschannen, Laurent Itti, and Anima Anandkumar. Born again neural networks. In *International Conference on Machine Learning*, pages 1607–1616. PMLR, 2018. 3
- [13] Shangqian Gao, Feihu Huang, Jian Pei, and Heng Huang. Discrete model compression with resource constraint for deep neural networks. *Proceedings of the IEEE/CVF Conference on Computer Vision and Pattern Recognition*, pages 1899–1908, 2020. 6
- [14] Shangqian Gao, Feihu Huang, Weidong Cai, and Heng Huang. Network pruning via performance maximization. *Proceedings of the IEEE/CVF Conference on Computer Vision and Pattern Recognition*, pages 9270–9280, 2021. 6
- [15] Ross Girshick. Fast r-cnn. In *Proceedings of the IEEE international conference on computer vision*, pages 1440–1448, 2015. 1
- [16] Ross Girshick, Jeff Donahue, Trevor Darrell, and Jitendra Malik. Rich feature hierarchies for accurate object detection and semantic segmentation. In *IEEE International Conference on Computer Vision (ICCV)*, pages 580–587, 2014. 1
- [17] Akhilesh Gotmare, Nitish Shirish Keskar, Caiming Xiong, and Richard Socher. A closer look at deep learning heuristics: Learning rate restarts, warmup and distillation. In *International Conference on Learning Representations*, 2019. 3
- [18] Raia Hadsell, Sumit Chopra, and Yann LeCun. Dimensionality reduction by learning an invariant mapping. In *2006 IEEE computer society conference on computer vision and pattern recognition (CVPR'06)*, pages 1735–1742. IEEE, 2006. 3
- [19] Song Han, Jeff Pool, John Tran, and William Dally. Learning both weights and connections for efficient neural network. *Advances in neural information processing systems*, 28, 2015. 1, 3
- [20] Kaiming He, Xiangyu Zhang, Shaoqing Ren, and Jian Sun. Deep residual learning for image recognition. In *Proceedings of the IEEE conference on computer vision and pattern recognition*, pages 770–778, 2016. 1, 6
- [21] Kaiming He, Georgia Gkioxari, Piotr Dollár, and Ross Girshick. Mask r-cnn. In *Proceedings of the IEEE international conference on computer vision*, pages 2961–2969, 2017. 1
- [22] Yang He, Guoliang Kang, Xuanyi Dong, Yanwei Fu, and Yi Yang. Soft filter pruning for accelerating deep convolutional neural networks. In *International Joint Conference on Artificial Intelligence (IJCAI)*, pages 2234–2240, 2018. 2, 4, 6, 7
- [23] Yang He, Ping Liu, Ziwei Wang, Zhilan Hu, and Yi Yang. Filter pruning via geometric median for deep convolutional neural networks acceleration. In *Proceedings of the IEEE/CVF conference on computer vision and pattern recognition*, pages 4340–4349, 2019. 2, 3, 6, 7
- [24] Geoffrey Hinton, Oriol Vinyals, and Jeff Dean. Distilling the knowledge in a neural network. *arXiv preprint arXiv:1503.02531*, 2015. 1, 3
- [25] Duc NM Hoang, Shiwei Liu, Radu Marculescu, and Zhangyang Wang. Revisiting pruning at initialization through the lens of ramanujan graph. In *The Eleventh International Conference on Learning Representations*, 2022. 3

- [26] Zejiang Hou, Minghai Qin, Fei Sun, Xiaolong Ma, Kun Yuan, Yi Xu, Yen-Kuang Chen, Rong Jin, Yuan Xie, and Sun-Yuan Kung. Chex: Channel exploration for cnn model compression. In *Proceedings of the IEEE/CVF Conference on Computer Vision and Pattern Recognition*, pages 12287–12298, 2022. 2, 3, 6, 7
- [27] Ryan Humble, Maying Shen, Jorge Albericio Latorre, Eric Darve, and Jose Alvarez. Soft masking for cost-constrained channel pruning. In *European Conference on Computer Vision*, pages 641–657. Springer, 2022. 2, 3
- [28] Bailin Li, Bowen Wu, Jiang Su, and Guangrun Wang. Eagleeye: Fast sub-net evaluation for efficient neural network pruning. In *Computer Vision—ECCV 2020: 16th European Conference, Glasgow, UK, August 23–28, 2020, Proceedings, Part II 16*, pages 639–654. Springer, 2020. 6, 7
- [29] Yun Li, Zechun Liu, Weiqun Wu, Haotian Yao, Xiangyu Zhang, Chi Zhang, and Baoqun Yin. Weight-dependent gates for network pruning. *IEEE Transactions on Circuits and Systems for Video Technology*, 32(10):6941–6954, 2022. 6, 7
- [30] Lucas Liebenwein, Cenk Baykal, Harry Lang, Dan Feldman, and Daniela Rus. Provable filter pruning for efficient neural networks. *Proceedings of International Conference on Learning Representations*, 2020. 6
- [31] Mingbao Lin, Rongrong Ji, Yan Wang, Yichen Zhang, Baochang Zhang, Yonghong Tian, and Ling Shao. Hrank: Filter pruning using high-rank feature map. In *Proceedings of the IEEE/CVF conference on computer vision and pattern recognition*, pages 1529–1538, 2020. 1, 2, 3
- [32] Mingbao Lin, Yuxin Zhang, Yuchao Li, Bohong Chen, Fei Chao, Mengdi Wang, Shen Li, Yonghong Tian, and Rongrong Ji. 1xn pattern for pruning convolutional neural networks. *IEEE Transactions on Pattern Analysis and Machine Intelligence*, 45(4):3999–4008, 2023. 3
- [33] Xuezhe Ma, Yingkai Gao, Zhiting Hu, Yaoliang Yu, Yuntian Deng, and Eduard Hovy. Dropout with expectation-linear regularization. In *International Conference on Learning Representations*, 2017. 3
- [34] TorchVision maintainers and contributors. Torchvision: Pytorch’s computer vision library. <https://github.com/pytorch/vision>, 2016. 7
- [35] Asit Mishra, Jorge Albericio Latorre, Jeff Pool, Darko Stosic, Dusan Stosic, Ganesh Venkatesh, Chong Yu, and Paulius Micikevicius. Accelerating sparse deep neural networks. *arXiv preprint arXiv:2104.08378*, 2021. 3
- [36] Hossein Mobahi, Mehrdad Farajtabar, and Peter Bartlett. Self-distillation amplifies regularization in hilbert space. *Advances in Neural Information Processing Systems*, 33:3351–3361, 2020. 3
- [37] Pavlo Molchanov, Stephen Tyree, Tero Karras, Timo Aila, and Jan Kautz. Pruning convolutional neural networks for resource efficient inference. In *5th International Conference on Learning Representations, ICLR 2017, Toulon, France, April 24–26, 2017, Conference Track Proceedings*. OpenReview.net, 2017. 2, 3
- [38] Pavlo Molchanov, Arun Mallya, Stephen Tyree, Iuri Frosio, and Jan Kautz. Importance estimation for neural network pruning. In *Proceedings of the IEEE/CVF conference on computer vision and pattern recognition*, pages 11264–11272, 2019. 3, 6, 7
- [39] Xuefei Ning, Tianchen Zhao, Wenshuo Li, Peng Lei, Yu Wang, and Huazhong Yang. Dsa: More efficient budgeted pruning via differentiable sparsity allocation. In *European Conference on Computer Vision*, pages 592–607. Springer, 2020. 6
- [40] Adam Paszke, Sam Gross, Francisco Massa, Adam Lerer, James Bradbury, Gregory Chanan, Trevor Killeen, Zeming Lin, Natalia Gimelshein, Luca Antiga, et al. Pytorch: An imperative style, high-performance deep learning library. *Advances in neural information processing systems*, 32, 2019. 6
- [41] Hanyu Peng, Jiayang Wu, Shifeng Chen, and Junzhou Huang. Collaborative channel pruning for deep networks. In *International Conference on Machine Learning*, pages 5113–5122. PMLR, 2019. 3
- [42] Jeff Pool and Chong Yu. Channel permutations for n: M sparsity. *Advances in neural information processing systems*, 34:13316–13327, 2021. 3, 5
- [43] Yaguan Qian, Zhiqiang He, Yuqi Wang, Bin Wang, Xiang Ling, Zhaoquan Gu, Haijiang Wang, Shaoning Zeng, and Wassim Swaileh. Hierarchical threshold pruning based on uniform response criterion. *IEEE Transactions on Neural Networks and Learning Systems*, pages 1–13, 2023. 6, 7
- [44] Olga Russakovsky, Jia Deng, Hao Su, Jonathan Krause, Sanjeev Satheesh, Sean Ma, Zhiheng Huang, Andrej Karpathy, Aditya Khosla, Michael Bernstein, et al. Imagenet large scale visual recognition challenge. *International journal of computer vision*, 115(3):211–252, 2015. 6
- [45] Florian Schroff, Dmitry Kalenichenko, and James Philbin. Facenet: A unified embedding for face recognition and clustering. In *Proceedings of the IEEE conference on computer vision and pattern recognition*, pages 815–823, 2015. 3
- [46] Dinghan Shen, Mingzhi Zheng, Yelong Shen, Yanru Qu, and Weizhu Chen. A simple but tough-to-beat data augmentation approach for natural language understanding and generation. *arXiv preprint arXiv:2009.13818*, 2020. 3
- [47] Maying Shen, Pavlo Molchanov, Hongxu Yin, and Jose M Alvarez. When to prune? a policy towards early structural pruning. In *Proceedings of the IEEE/CVF Conference on Computer Vision and Pattern Recognition*, pages 12247–12256, 2022. 2
- [48] Patrice Y Simard, Yann A LeCun, John S Denker, and Bernard Victorri. Transformation invariance in pattern recognition—tangent distance and tangent propagation. In *Neural networks: tricks of the trade*, pages 239–274. Springer, 2002. 2, 3
- [49] Karen Simonyan and Andrew Zisserman. Very deep convolutional networks for large-scale image recognition. In *International Conference on Learning Representations (ICLR)*, 2015. 1
- [50] Xiu Su, Shan You, Tao Huang, Fei Wang, Chen Qian, Changshui Zhang, and Chang Xu. Locally free weight sharing for network width search. In *International Conference on Learning Representations*, 2021. 7
- [51] Yijun Tan, Kai Han, Kang Zhao, Xianzhi Yu, Zidong Du, Yunji Chen, Yunhe Wang, and Jun Yao. Accelerating sparse

- convolution with column vector-wise sparsity. *Advances in Neural Information Processing Systems*, 35:30307–30317, 2022. 3
- [52] Yehui Tang, Yunhe Wang, Yixing Xu, Dacheng Tao, Chun-jing Xu, Chao Xu, and Chang Xu. Scop: Scientific control for reliable neural network pruning. *Proceedings of Advances in Neural Information Processing Systems*, 2020. 6
- [53] Huan Wang and Yun Fu. Trainability preserving neural pruning. In *The Eleventh International Conference on Learning Representations*, 2023. 6
- [54] Yandong Wen, Kaipeng Zhang, Zhifeng Li, and Yu Qiao. A discriminative feature learning approach for deep face recognition. In *Computer Vision—ECCV 2016: 14th European Conference, Amsterdam, The Netherlands, October 11–14, 2016, Proceedings, Part VII 14*, pages 499–515. Springer, 2016. 3
- [55] Lijun Wu, Juntao Li, Yue Wang, Qi Meng, Tao Qin, Wei Chen, Min Zhang, Tie-Yan Liu, et al. R-drop: Regularized dropout for neural networks. *Advances in Neural Information Processing Systems*, 34:10890–10905, 2021. 3, 4
- [56] Ting-Bing Xu and Cheng-Lin Liu. Data-distortion guided self-distillation for deep neural networks. In *Proceedings of the AAAI Conference on Artificial Intelligence*, pages 5565–5572, 2019. 3
- [57] H Zhang, M Cisse, Y Dauphin, and D Lopez-Paz. mixup: Beyond empirical risk management. In *Proc. 6th Int. Conf. Learn. Represent.(ICLR)*, pages 1–13, 2018. 7
- [58] Linfeng Zhang, Jiebo Song, Anni Gao, Jingwei Chen, Chenglong Bao, and Kaisheng Ma. Be your own teacher: Improve the performance of convolutional neural networks via self distillation. In *Proceedings of the IEEE/CVF international conference on computer vision*, pages 3713–3722, 2019. 3
- [59] Xiangyu Zhang, Xinyu Zhou, Mengxiao Lin, and Jian Sun. Shufflenet: An extremely efficient convolutional neural network for mobile devices. In *Proceedings of the IEEE conference on computer vision and pattern recognition*, pages 6848–6856, 2018. 1
- [60] Ying Zhang, Tao Xiang, Timothy M Hospedales, and Huchuan Lu. Deep mutual learning. In *Proceedings of the IEEE conference on computer vision and pattern recognition*, pages 4320–4328, 2018. 3, 4
- [61] Yuxin Zhang, Mingbao Lin, Chia-Wen Lin, Jie Chen, Yongjian Wu, Yonghong Tian, and Rongrong Ji. Carrying out cnn channel pruning in a white box. *IEEE Transactions on Neural Networks and Learning Systems*, 2022. 6, 7
- [62] Chuanyang Zheng, Kai Zhang, Zhi Yang, Wenming Tan, Jun Xiao, Ye Ren, Shiliang Pu, et al. Savit: Structure-aware vision transformer pruning via collaborative optimization. *Advances in Neural Information Processing Systems*, 35:9010–9023, 2022. 3
- [63] Konrad Zolna, Devansh Arpit, Dendi Suhubdy, and Yoshua Bengio. Fraternal dropout. In *International Conference on Learning Representations*, 2018. 3